Title

PSF reconstruction for AO photometry and astrometry

Journal

Adaptive Optics for Extremely Large Telescopes 4 – Conference Proceedings, 1(1)

Authors

Ascenso, Joana
Neichel, Benoit
Silva, Manuel
et al.

Publication Date

2015

DOI

10.20353/K3T4CP1131540

PSF reconstruction for AO photometry and astrometry

Joana Ascenso[a,b], Benoit Neichel[c], Manuel Silva[a], Thierry Fusco[c,d], and Paulo Garcia[a,b]

[a]CENTRA, Pavilhão de Física, Av. Rovisco Pais 1, 1049-001 Lisboa, Portugal
[b]Universidade do Porto, Faculdade de Engenharia, Rua Dr. Roberto Frias, s/n, P-4200-465 Porto, Portugal
[c]Aix Marseille Universit, CNRS, LAM (Laboratoire d'Astrophysique de Marseille) UMR 7326, 13388, Marseille, France
[d]ONERA, BP 72, F-92322 Chatillon, France

ABSTRACT

Extracting accurate photometry (and astrometry) from images taken with adaptive optics assisted instruments is particularly challenging. Current post-processing tools are not prepared to achieve high accuracy from AO data, especially in limiting cases of crowded fields and marginally resolved sources. We quantify the limitations of these tools with synthetic images, and present a proof-of-concept study showing the potential of using reconstructed PSFs from the (GL)AO system telemetry to increase the measured photometric accuracy. We show that the photometric accuracy is significantly improved with a good PSF reconstruction in considerably crowded regions. We demonstrate the need for a dedicated post-processing tool that incorporates available information about the PSF, as well as the ability to adjust to the spatial variations of the PSF characteristic of AO data.

1. INTRODUCTION

Photometry and astrometry (fluxes and positions) are the basis for all astrophysical applications of observational imaging data, regardless of the area of research. Multi-band photometric measurements of stellar sources allow time efficient determinations of their luminosities, effective temperatures, masses, and even ages. For faint sources, beyond the sensitivity limits for spectroscopy, photometry is the only way to estimate these quantities.[1] Extinction maps derived from photometric measurements of field stars provide the most robust representation of the mass distribution of molecular clouds, the sites of star formation.[2] High-precision, time-resolved photometry light curves reveal a wealth of information on the structure and evolution of stars (e.g. asteroseismology) and of transiting planet candidates.[3] For several of these planets, the same photometric observations also give insight to their density and even composition. Accurate astrometry probes absolute motions perpendicular to the line-of-sight and absolute parallaxes. Astrometric distances are the fundamental calibrators of the cosmological distance scale and of all methods for deriving the luminosity of astrophysical sources from their apparent brightness.[4]

Adaptive optics (AO) systems were devised to enhance the resolution and sensitivity of telescopes, pushing the boundaries of the science to limits that were fundamentally barred with seeing-limited observations. AO systems correct the wavefront distortions introduced by turbulence from the Earth's atmosphere in the optical path of astronomical observations.[5] The resulting images have higher resolution than seeing-limited images by a factor of a few, introducing a significant advantage of AO over non-AO instruments and bringing the telescopes closer to their full potential to produce diffraction-limited images. This is such that most large observatories existing now and planned for the foreseeable future are being upgraded or designed to include AO systems in their baseline configurations. The downside of these systems is that the correction of the wavefront distortions is not perfect: since the wavefront is sensed using one or several reference star(s), the correction is optimal toward the reference axis and degrades away from this (these) point(s). As a consequence, AO images show a PSF (point spread function) that is variable on scales larger than a few arcseconds.[6] The magnitude and characteristics of the spatial PSF variations depend on several parameters, namely on the point-like nature and brightness of the reference star, but mostly they depend on the AO flavour of the system (SCAO, MCAO, MOAO, etc.). Ground

Further author information: (Send correspondence to J.A.)
J.A.: E-mail:jascenso@fe.up.pt

layer AO (GLAO) in particular corrects for the ground turbulent boundary layer over large fields of view; the correction is poorer with respect to other AO systems but it is more stable across the field of view.

Naturally, the post-processing of AO data, including photometry and astrometry, is a critical step to extract meaningful scientific information. However, the currently available tools for photometry and astrometry are best suited for traditional, seeing-limited data, obtained by telescopes without correction for atmospheric turbulence. In seeing-limited images the PSF can be well described by a simple analytic function like a Gaussian or a Lorentzian. Furthermore, provided the field is not too large, the PSF is constant across the field of view, or slowly varying at worse. In these data, the extraction of photometry and astrometry for point sources to the accuracy required for science is a relatively straightforward and direct problem that has several satisfactory solutions. But AO systems produce PSFs that are no longer well described by simple analytical functions, rather presenting sharp cores, diffraction rings and extended (faint) wings that vary rapidly in time and across the field. Current tools can be and frequently are used in AO data with acceptable results, but it is not clear that they harvest the full potential of adaptive optics.

1.1 Existing post-processing tools

There are three main tools to extract photometry from astronomical images: DAOPHOT,[7] Starfinder,[8] and SExtractor.[9] We will focus on the first two in the current work.

DAOPHOT is a tool developed for seeing-limited data and works by fitting an analytical model plus some residual tables to the point sources in an image. The functions are chosen to match observed, seeing-limited PSFs, and the residuals are estimated from selected reference stars in the image. DAOPHOT offers the interesting possibility of adding a spatial variability term to the residuals to account for variations of the PSF in the field; currently variations can be mapped as a polynomial. The accuracy of the fit depends crucially on the availability of adequate PSF reference stars: they should be bright (high signal-to-noise ratio), isolated, to avoid contamination from neighbouring stars, and evenly distributed in the field, to probe the full scale of PSF variations. This limits its applicability to fields where such stars exist, leaving out crowded fields, and sparse fields whose objects of interest are just barely resolved.

Starfinder is an algorithm built specifically for isoplanatic AO PSF: it estimates the model of the PSF completely from either a user-selected sample of suitable stars in the image, or iteratively using all stars in the image rather than assuming the PSF is well described by an analytical function. Also, it has the interesting feature that it allows the user to input a PSF model to be fitted to the sources in the image. Its main limitation is that it assumes a constant PSF, which significantly hampers its performance on AO data with fields of view larger than the isoplanatic patch. A workaround consisting on dividing the field into small regions where the PSF is stable has been proposed, but this is not an ideal solution since it requires there be enough stars to define the PSF in all sub-regions, and also introduces a zeropoint shift between sub-regions that could decrease the accuracy of the photometry by an important amount.

In this work we compare the performance of DAOPHOT and Starfinder using a controlled set of syntetic (GL)AO data (section 2), and investigate the added value of using reconstructed PSFs from the telemetry of the AO system as the model PSF for each image (section 3.2). We present our preliminary conclusions in section 4.

2. SYNTHETIC IMAGES

To compare the performance of currently available tools for photometry it is necessary to have a controlled dataset. We have produced synthetic AO images using the Gemini/GEMS system in GLAO mode as reference and the Yao software.[10] In this report we present the results only for the best simulated conditions ($r_0 = 0.122$ m and a typical C_n^2 profile). For this setup the average FWHM (full width at half maximum) of the PSF is around 4 pixels.

The images have an ∼80”× 80” field of view (∼4000 × 4000 pixels), and contain 5374 stars distributed spatially according to a King[11] profile. This distribution produces a gradient of stellar density from the centre to the peripheries of the images, allowing us to assess the effectiveness of the tools in different crowding levels.

The brightness of each star was obtained by randomly sampling from a normal initial mass function[12] and assuming a mass-luminosity relation for the K band[13] for a 2 million year population, a distance of 3 kpc, and no interstellar extinction. The stars' brightness in the synthetic images ranged from 5.4 to 19.0 magnitudes. We did not include the effects of saturation, but we limited the detection of sources to the linearity limit of GEMS. 17 bright isolated stars were artificially added to make sure there were adequate PSF reference stars. The full study will present the results obtained for the limiting case of few or no suitable PSF reference stars.

We added a sky background and photon noise expected for GEMS's detector to the images, and the sky was then subtracted from the final images, mimicking the procedure adopted in real observations. The results described in this report refer to images with a high signal-to-noise ratio.

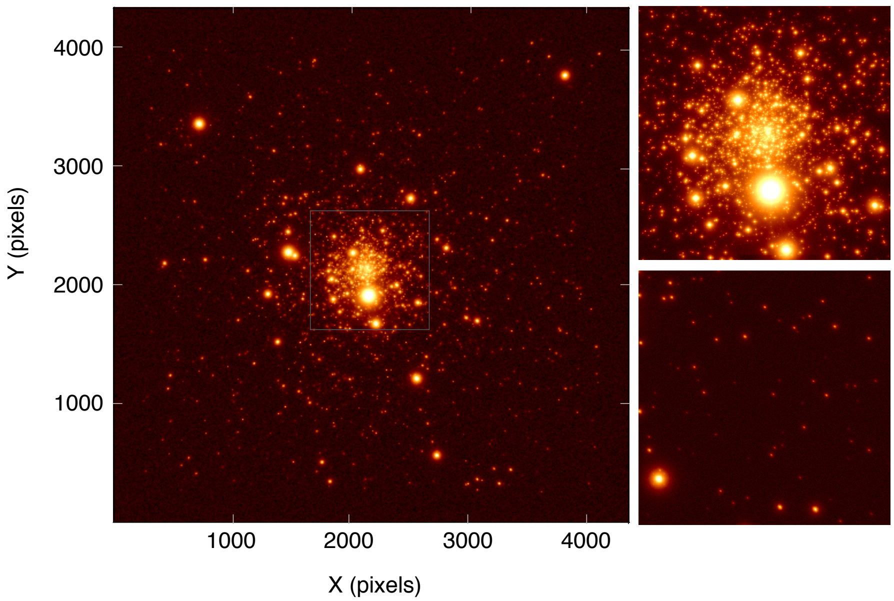

Figure 1. Example of a synthetic AO image used to assess the performance of the existing post-processing tools. The right panels show the detail of the centre (top) and the periphery (bottom) of the image, illustrating the different degrees of crowding, and also the more elongated PSF in the latter.

Figure 1 shows an example of a synthetic image in logarithmic intensity scale. It is easily seen that the images cover a wide range of source crowding conditions, allowing us to assess the performance of DAOPHOT and Starfinder in these different conditions. Also shown in the figure (bottom right) is the elongation of the PSF in the lower right corner of the image, illustrating the PSF variations observed across the field. The positions of the synthetic laser and natural guide stars are such that the distortions are approximately radial.

3. ANALYSIS AND RESULTS

To quantify the performance of currently existing tools in AO data we have done PSF photometry using DAOPHOT and Starfinder on our synthetic images. Since we know exactly the brightness of the stars in our images, the difference between the input and the measured photometry, Δmag, provides an estimate of the photometric accuracy. Here we describe the results for a good signal-to-noise image with a good AO correction, and with a fair number of PSF reference stars.

3.1 DAOPHOT

For this analysis we used the DAOPHOT implementation in IRAF v2.16.1.

The procedure for the PSF photometry involves detecting the stars, doing aperture photometry, estimating the PSF (in practice defining the residual tables with respect to the analytical function profile), and fitting the PSF to extract the final photometry. Since the PSF reference stars were artificially clean of neighbours, it was not necessary to run DAOPHOT iteratively to define the PSF. After experimenting with different values, we used a fitting radius of 5 pixels, comparable to the average FWHM in the image, and a PSF radius of 30 pixels to properly account for the extended wings of the PSF. The analytical function that best fit the image PSFs was a Lorentz function.

To assess the importance of allowing the PSF to vary in the field, we first ran DAOPHOT using a constant (order 0 polynomial) PSF in the field, and then increased the order of the residual-mapping polynomial to 2. The latter is equivalent to letting the residuals adjust as a quadratic function of position in the image. Figure 2 shows Δmag for DAOPHOT order 0 (constant PSF, left), and for DAOPHOT order 2 (variable PSF, right), both in a 3D plot for a visual perspective (top), and in a scatter plot (bottom).

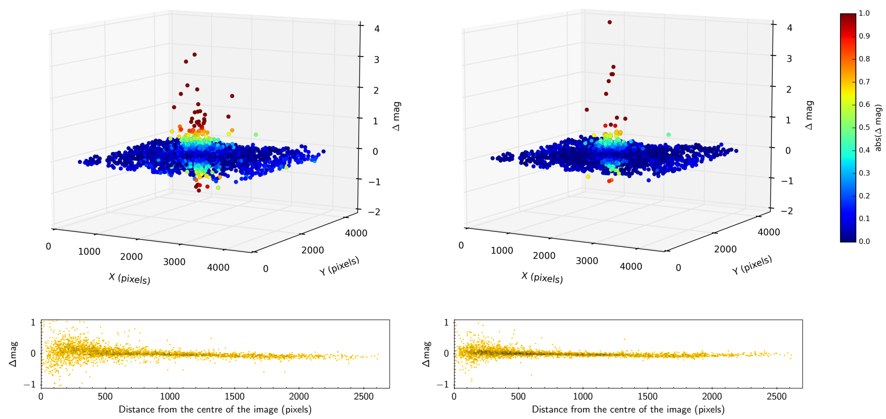

Figure 2. Difference (Δmag) between input magnitudes and magnitudes measured with DAOPHOT for the stars in the synthetic image. Top: position-position-Δmag plots. Bottom: scatter plots of Δmag as a function of distance from the image centre. Left: results from the order 0/constant PSF test. Right: results from the order 2/variable PSF test. See text for more details.

It is clear that a variable PSF provides more accurate photometry than the constant PSF model, both on a global scale and also in the challenging crowded centre. The dispersion of Δmag is 0.22 mag for the constant PSF case, and 0.16 mag for the photometry using a variable PSF. This represents an improvement in accuracy of 30% globally relative to the constant PSF. Considering that these results are for images from a (synthetic) GLAO system, that produces relatively small field distortions, it is expected that the improvement be even more significant in the more extreme cases of SCAO or MCAO. This illustrates the importance of having a tool that allows the PSF to vary in the field to extract accurate photometry from AO observations.

Despite the clear advantages of using a variable over a constant PSF for photometry, the intrinsic accuracy of the photometry, especially for the moderately to severely crowded regions, is far from ideal: even with the variable PSF, the average photometric error in the inner 500 pixel radius is above 20%. This value is valid only for this particular instrumental setup and stellar density, but it shows that the PSF model used to extract the photometry in the centre is not good enough. Although it is possible to obtain excellent results with DAOPHOT even in crowded regions (see e.g., P. Turri, these proceedings), it is at the expense of an impractical amount of iterative effort that precludes the processing of a reasonable number of images in a timely or semi-automated manner.

3.2 Starfinder

We used equivalent parameters to those described in the previous section to extract photometry of the point sources using Starfinder. We did three classes of tests with Starfinder.

The baseline test was to allow Starfinder to define the PSF iteratively from the image and the source list it detected; this allowed us to assess the global performance of a typical run with Starfinder. The results are shown in Figure 3 (left). Starfinder performs well in a small part of the image (where the estimated PSF is close to the actual PSF), but since the PSF is not allowed to vary in the field, it underperforms significantly outside this region. The dependence of Δmag with distance to the centre of the image reflects the radial dependence of the PSF distortions in the image.

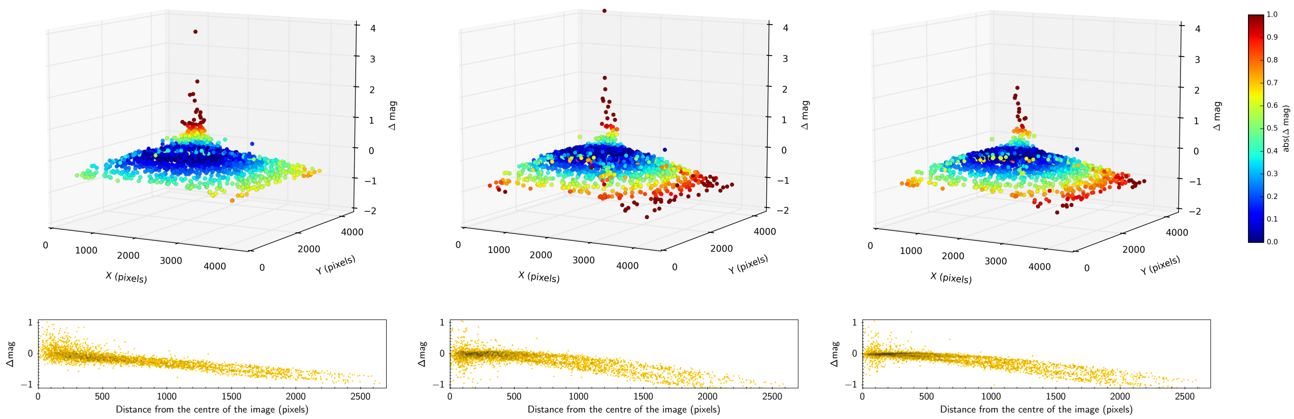

Figure 3. Difference (Δmag) between input magnitudes and magnitudes measured with Starfinder for the stars in the synthetic image. Top: position-position-Δmag plots. Bottom: scatter plots of Δmag as a function of distance from the image centre. Left: results from the first test (model PSF estimated from the image). Middle: results from the second test (model PSF = reconstructed PSF). Right: results from the third test (model PSF = true PSF). See text for more details.

In the second test we assessed the benefit of using a PSF reconstructed from the AO system telemetry (see M. Silva et al., these proceedings, for details on the PSF reconstruction) as the PSF model for the fit. We used Starfinder's feature that allows the user to upload a PSF model. Since Starfinder does not allow the PSF to vary in the field, we chose to reconstruct the PSF just slightly off the crowded centre, at position (2062, 2154) pixels in the detector. For the proof-of-concept study described here the PSF was reconstructed with the exact knowledge of the atmospheric profile used for the synthetic "observations". For this ideal case, the results are shown in Figure 3 (middle). Although it is not obvious that there was any improvement with respect to the PSF estimated by Starfinder, the scatter plots show a narrower distribution of Δmag around the position for which the PSF was reconstructed. To quantify that further, Table 1 shows the 1-σ dispersion of Δmag within a 200 pixel radius around that position for this test (PSFr) in comparison with the same quantity for the PSF estimated from the image by Starfinder (PSFi), showing that there is an appreciable improvement, especially considering that this is a very high stellar density region. Using the reconstructed PSF we achieved a 70% increase of accuracy in the 200 pixel around its position, corresponding to an average photometric accuracy of the order of 5% in this region. As expected, the relative gain degrades as we move away from this position because the PSF distortions in the field are not accounted for.

Table 1. Dispersion of Δmag on a 200 pixel radius around the position of the reconstructed PSF.

Starfinder run	$\sigma_{\Delta\mathrm{mag}}$
PSFi	0.18
PSFr	0.05
PSFt	0.02

The third test served to estimate the limit of improvement that could be achieved in photometric accuracy if the PSF reconstruction were perfect. We uploaded the actual PSF used to produce the synthetic images as PSF model to Starfinder; we used the same position as before such that the comparison would be straightforward. Table 1 shows the dispersion of Δmag within a 200 pixel radius around the reference position also for this test (PSFt). The photometric accuracy is now at the 2% level for this particular image and setup, which represents an improvement of almost 90% relative to the photometry for the same stars using the PSF model derived automatically by Starfinder.

4. CONCLUSIONS

We presented a proof-of-concept study meant to assess the adequacy of currently existing tools to derive accurate photometry from AO data, and the potential of using reconstructed PSFs to improve that accuracy. Although the exact numbers presented here are only valid for the characteristics of the image and AO setup we chose to simulate, they illustrate three important points:

- Currently existing tools do not harvest the full potential of AO-assisted data. Although DAOPHOT performs well if there are (enough) adequate PSF reference stars in the image from which to characterise the PSF and map its variations in the field, it underperforms in regions where the PSF is ill-characterised. This is a potentially severe limitation for very crowded regions and small fields of view. Starfinder has the same limitation with the disadvantage that it does not allow the PSF to vary in the field, therefore producing worse results.
- The ability to adjust the PSF model to the spatial distortions characteristic of AO-corrected data is crucial in achieving accurate photometry. DAOPHOT performs well in mapping these distortions (for the case of GLAO) with an order 2 polynomial, and in translating the mapping into the PSF fit, provided that enough PSF stars are distributed in the field.
- The use of a reconstructed PSF as the PSF model for the photometry shows promising potential to significantly improve the photometric accuracy of AO-corrected data.

The current study argues strongly for the need of a new PSF-fitting tool for photometry (and astrometry) that combines the possibility of a field-varying PSF with all available information regarding the PSF.

In an upcoming paper we will describe the analysis and setup more thoroughly, and we will extend our results to a wider parameter space. In particular, we will assess the impact of the signal-to-noise ratio of the images, of the quality of the AO correction, of the atmosphere turbulence profile, and of the goodness of the PSF reconstruction on the photometric accuracy. We will also evaluate the limiting cases for which current tools are unsuitable or provide low photometric accuracy.

ACKNOWLEDGMENTS

The research leading to these results has received funding from the European Community's Seventh Framework Programme under Grant Agreement 312430 (OPTICON). J. A. acknowledges funding from FCT grant SFRH/BPD/101562/2014.

REFERENCES

[1] Straižys, V., [*Multicolor stellar photometry*] (1992).

[2] Alves, J., Lombardi, M., and Lada, C. J., "The mass function of dense molecular cores and the origin of the IMF," *Astronomy and Astrophysics* **462**, L17–L21 (Jan. 2007).

[3] Borucki, W. J., Koch, D., Basri, G., Batalha, N., Brown, T., Caldwell, D., Caldwell, J., Christensen-Dalsgaard, J., Cochran, W. D., DeVore, E., Dunham, E. W., Dupree, A. K., Gautier, T. N., Geary, J. C., Gilliland, R., Gould, A., Howell, S. B., Jenkins, J. M., Kondo, Y., Latham, D. W., Marcy, G. W., Meibom, S., Kjeldsen, H., Lissauer, J. J., Monet, D. G., Morrison, D., Sasselov, D., Tarter, J., Boss, A., Brownlee, D., Owen, T., Buzasi, D., Charbonneau, D., Doyle, L., Fortney, J., Ford, E. B., Holman, M. J., Seager, S., Steffen, J. H., Welsh, W. F., Rowe, J., Anderson, H., Buchhave, L., Ciardi, D., Walkowicz, L., Sherry, W., Horch, E., Isaacson, H., Everett, M. E., Fischer, D., Torres, G., Johnson, J. A., Endl, M., MacQueen, P., Bryson, S. T., Dotson, J., Haas, M., Kolodziejczak, J., Van Cleve, J., Chandrasekaran, H., Twicken, J. D., Quintana, E. V., Clarke, B. D., Allen, C., Li, J., Wu, H., Tenenbaum, P., Verner, E., Bruhweiler, F., Barnes, J., and Prsa, A., "Kepler Planet-Detection Mission: Introduction and First Results," *Science* **327**, 977 (Feb. 2010).

[4] Kovalevsky, J. and Seidelmann, P. K., [*Fundamentals of Astrometry*] (June 2004).
[5] Davies, R. and Kasper, M., "Adaptive Optics for Astronomy," *Annual Review of Astronomy and Astrophysics* **50**, 305–351 (Sept. 2012).
[6] Fusco, T., Conan, J.-M., Mugnier, L. M., Michau, V., and Rousset, G., "Characterization of adaptive optics point spread function for anisoplanatic imaging. Application to stellar field deconvolution," *Astronomy and Astrophysics Supplement* **142**, 149–156 (Feb. 2000).
[7] Stetson, P. B., "DAOPHOT - A computer program for crowded-field stellar photometry," *Publications of the ASP* **99**, 191–222 (Mar. 1987).
[8] Diolaiti, E., Bendinelli, O., Bonaccini, D., Close, L., Currie, D., and Parmeggiani, G., "Analysis of isoplanatic high resolution stellar fields by the StarFinder code," *Astronomy and Astrophysics Supplement* **147**, 335–346 (Dec. 2000).
[9] Bertin, E., "Automated Morphometry with SExtractor and PSFEx," in [*Astronomical Data Analysis Software and Systems XX*], Evans, I. N., Accomazzi, A., Mink, D. J., and Rots, A. H., eds., *Astronomical Society of the Pacific Conference Series* **442**, 435 (July 2011).
[10] Rigaut, F. and Van Dam, M., "Simulating Astronomical Adaptive Optics Systems Using Yao," in [*Proceedings of the Third AO4ELT Conference*], Esposito, S. and Fini, L., eds., 18 (Dec. 2013).
[11] King, I., "The structure of star clusters. I. an empirical density law," *Astronomical Journal* **67**, 471–+ (Oct. 1962).
[12] Kroupa, P., "On the variation of the initial mass function," *Monthly Notices of the Royal Astronomical Society* **322**, 231–246 (Apr. 2001).
[13] Ascenso, J., Alves, J., and Lago, M. T. V. T., "No evidence of mass segregation in massive young clusters," *Astronomy and Astrophysics* **495**, 147–155 (Feb. 2009).